THE STRONG EARTHQUAKES IN KHATANBULAG, DORNOGOBI PROVINCE

G.Bolormaa, D.Ganzorig, M. Oyun-Erdene, D. Khongor

Bolormaa.g@iag.ac.mn

Institute of Astronomy and Geophysics, MAS

ULAANBAATAR
2025.08.11

Outline

- Mongolian seismicity
  - Seismicity of Dornogobi province
  - Khatanbulag Area
    - iLoc relocation processing
      - Focal mechanism Main and Large aftershock
      - Magnitude calculation of Source Spectrum
- Conclusion

Institute of Astronomy and Geophysics

Mongolian seismicity

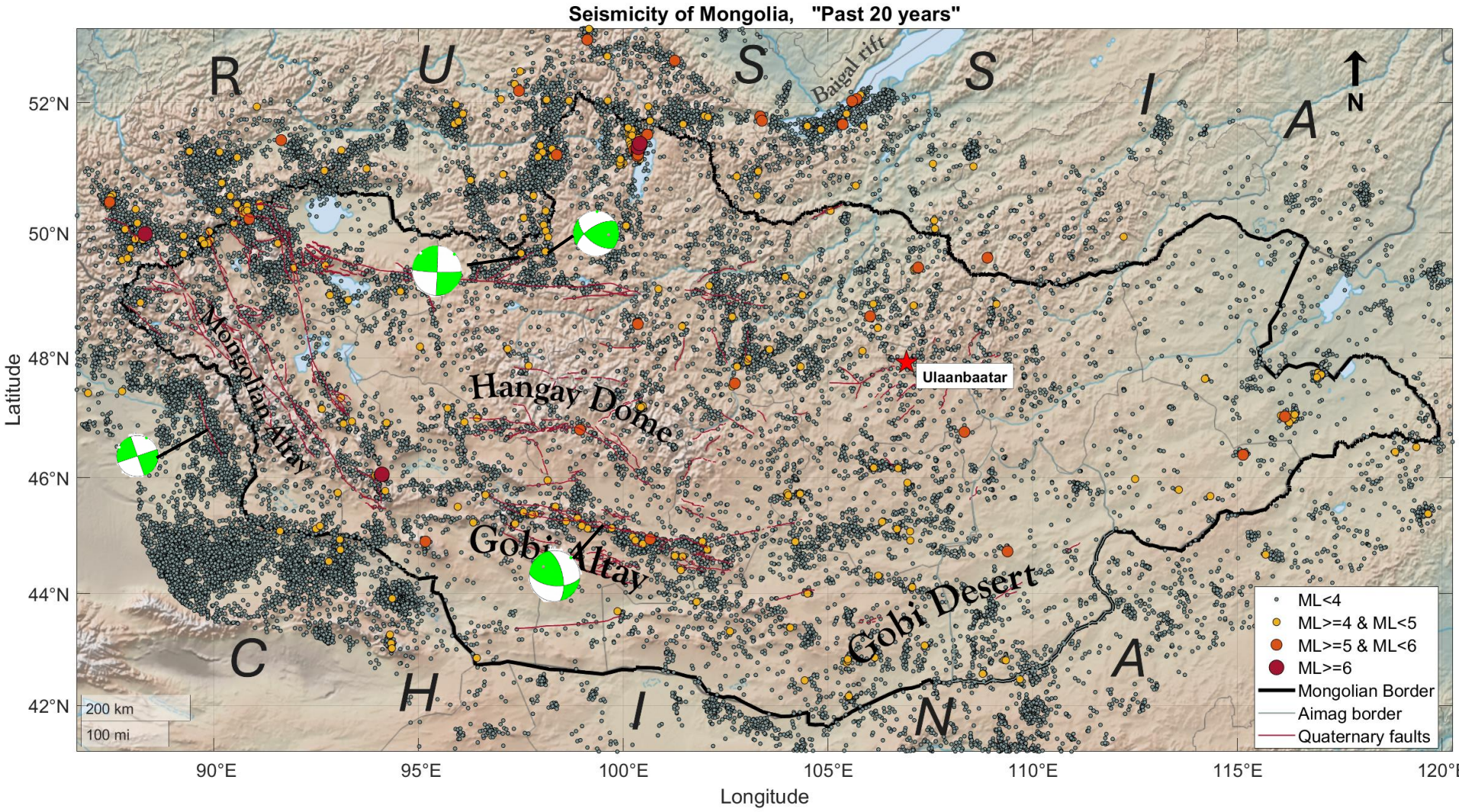

Figure:1. MNDC data 2025

Institute of Astronomy and Geophysics

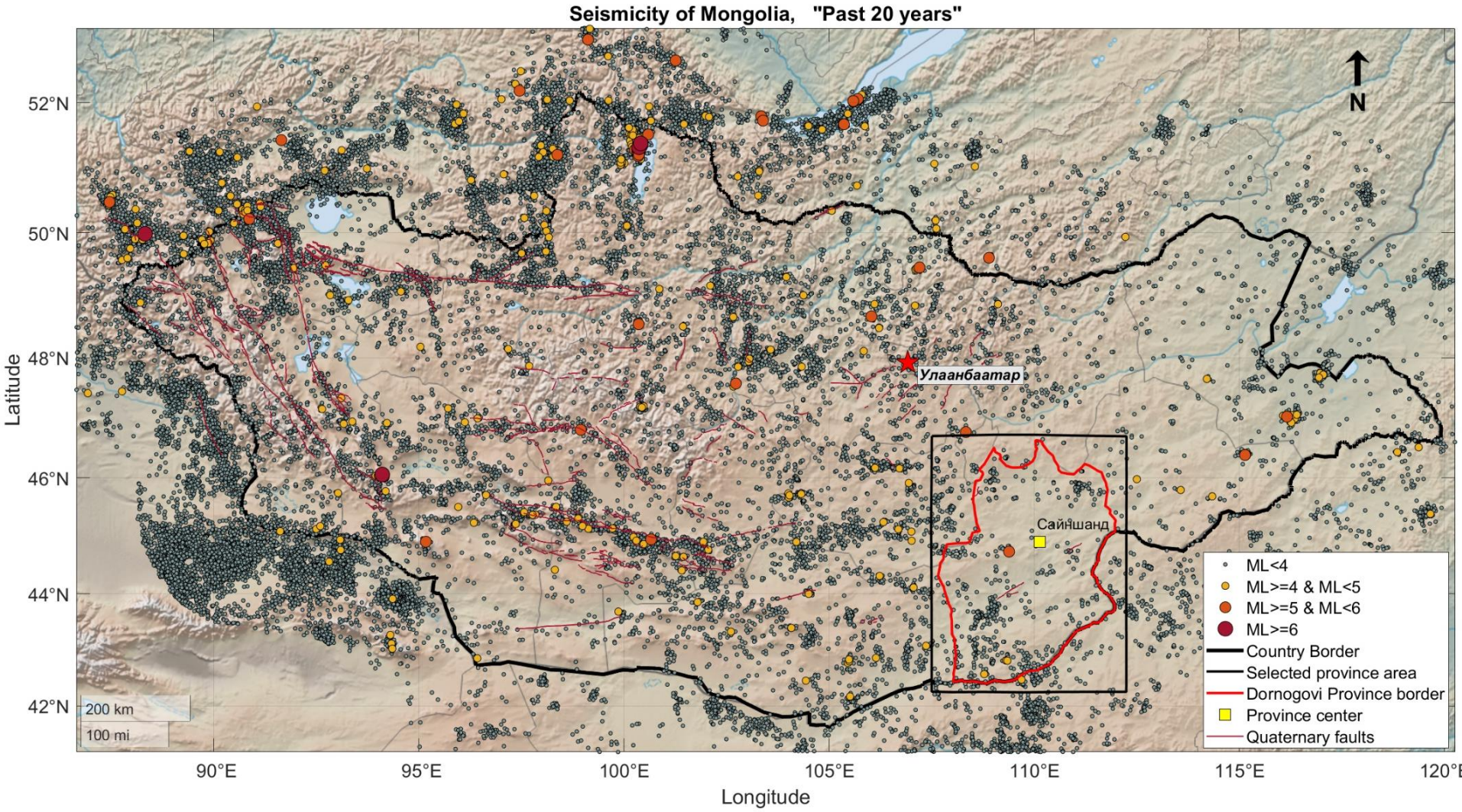

Institute of Astronomy and Geophysics

Seismicity of Dornogobi province

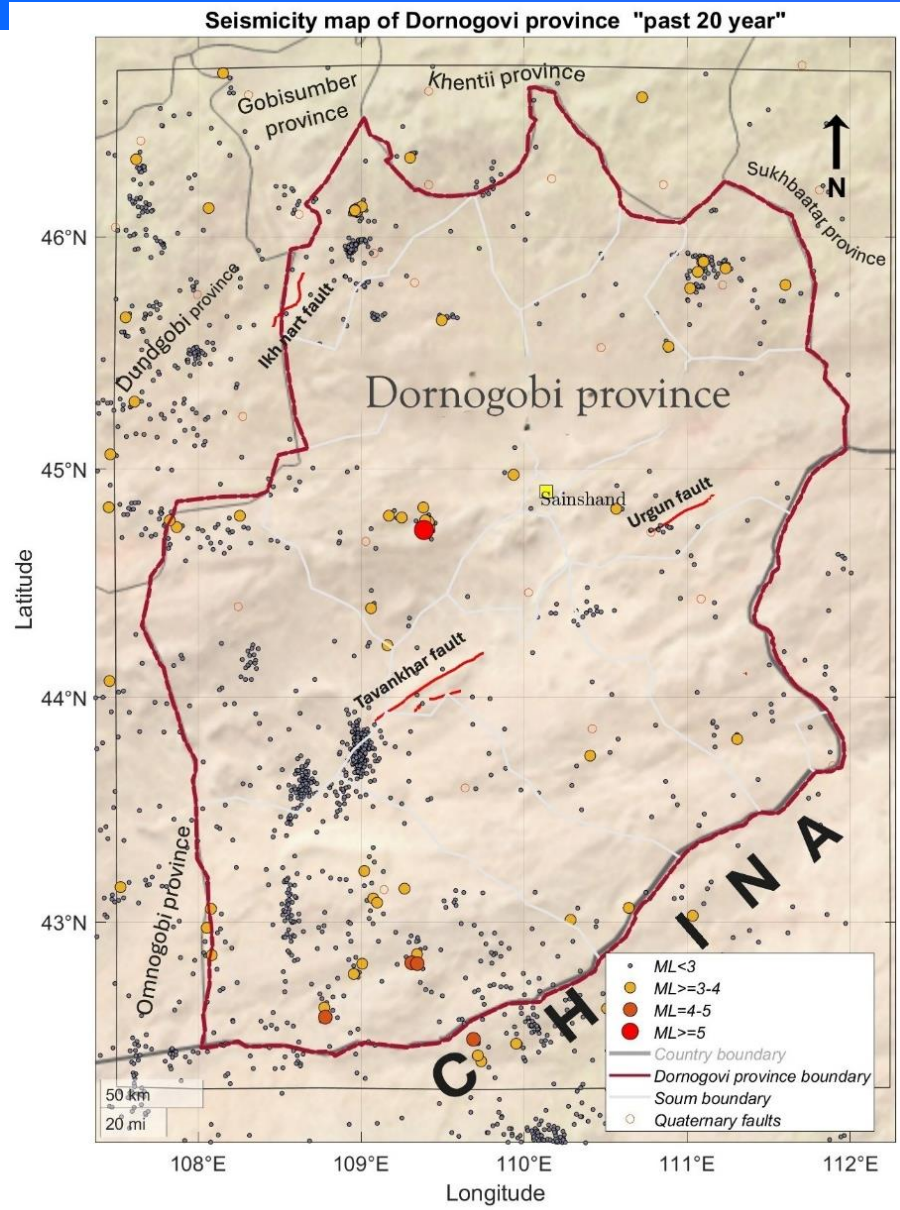

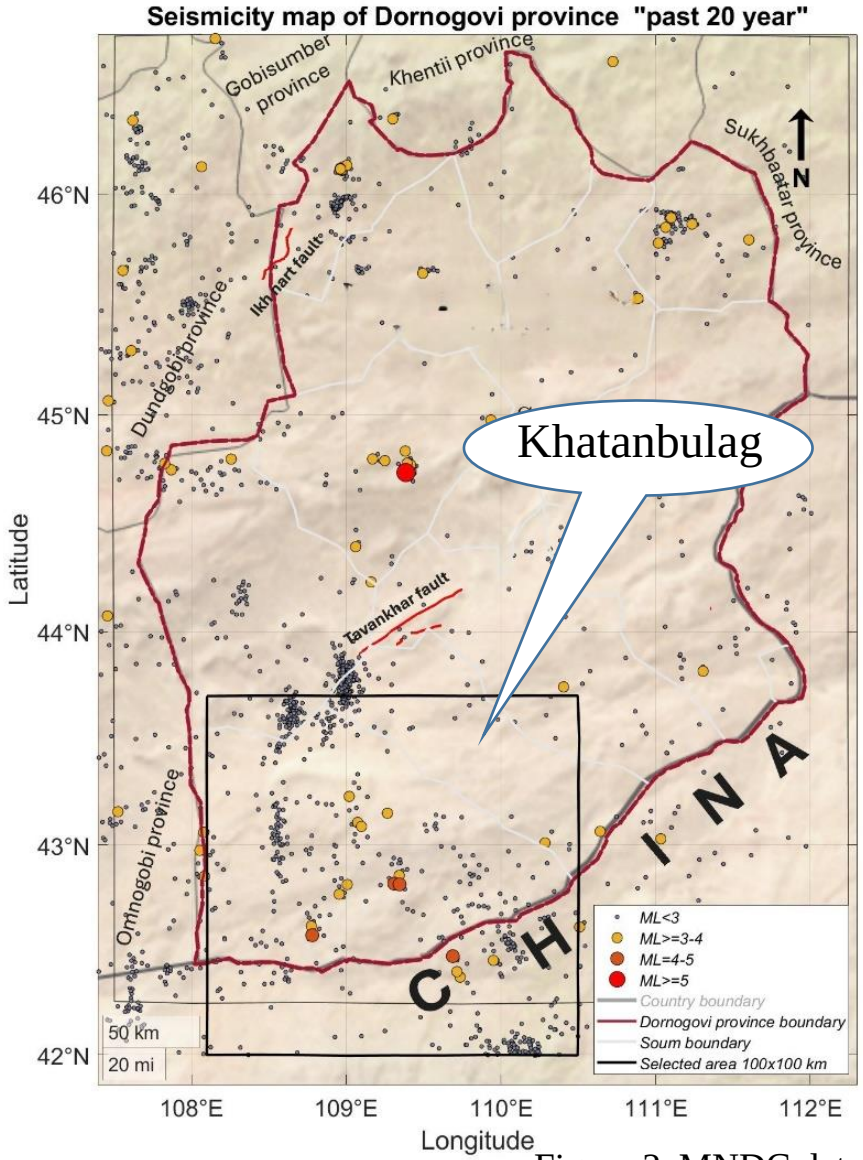

Figure:2. MNDC data 2025

Khatanbulag Area

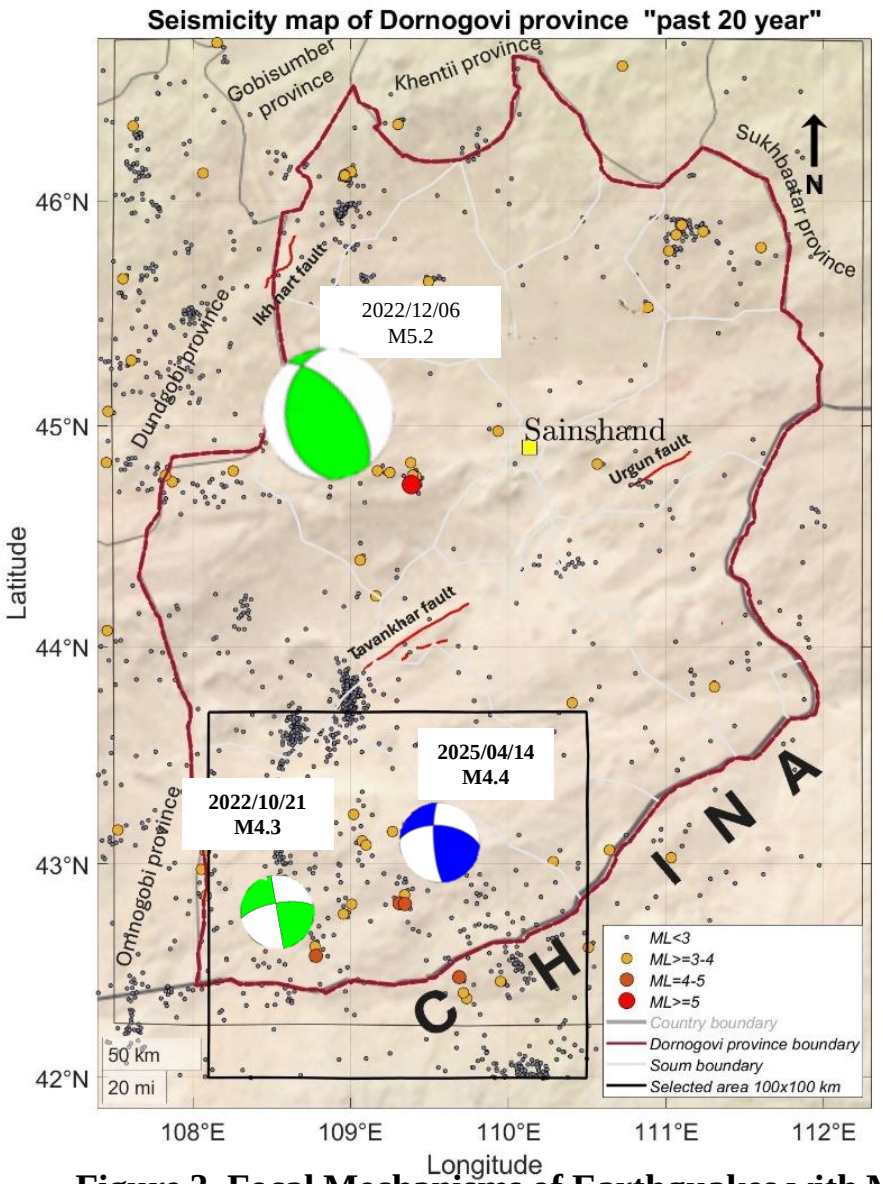

Figure 3. Focal Mechanisms of Earthquakes with ML ≥ 3.5 in the Khatanbulag Area

iLoc relocation

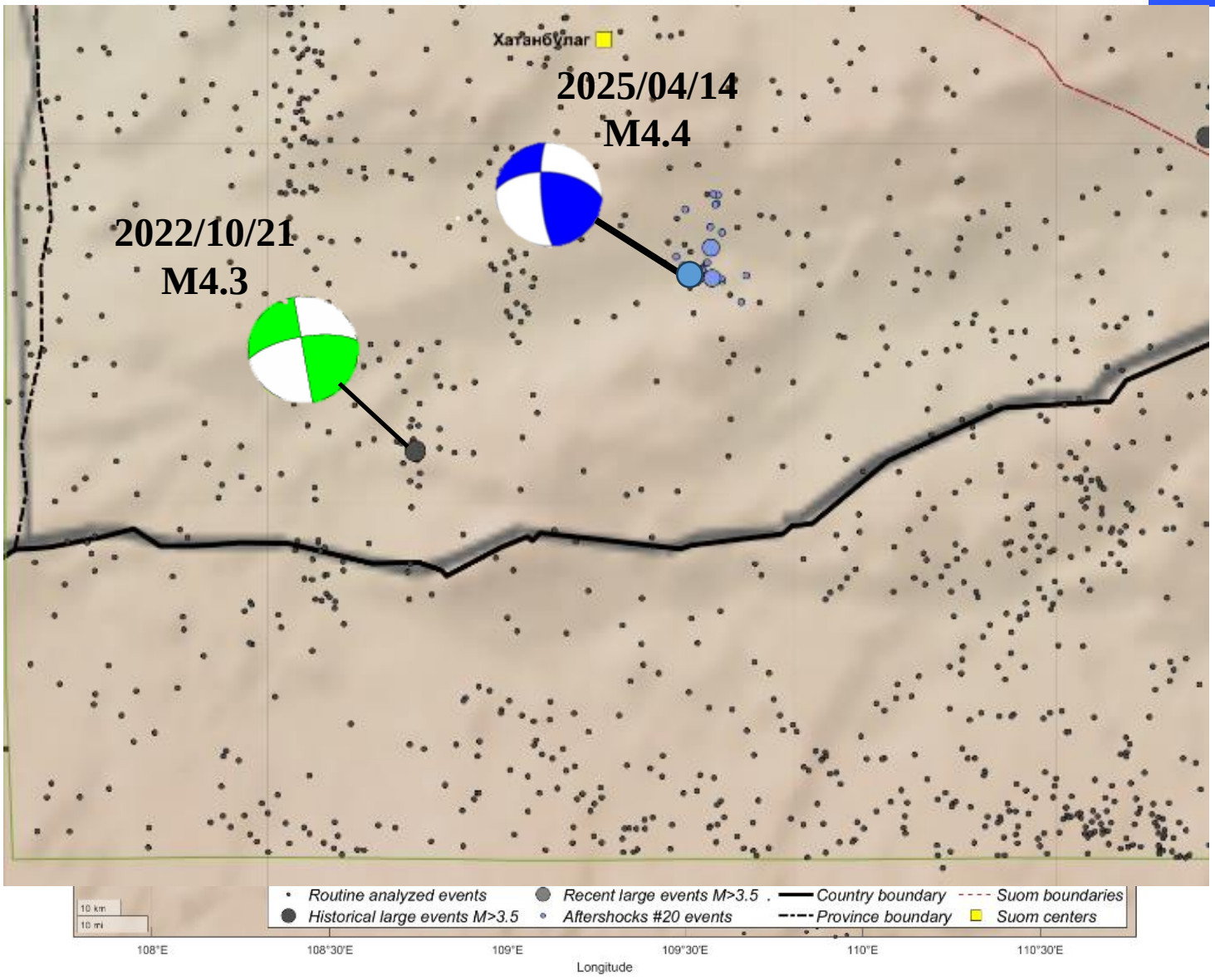

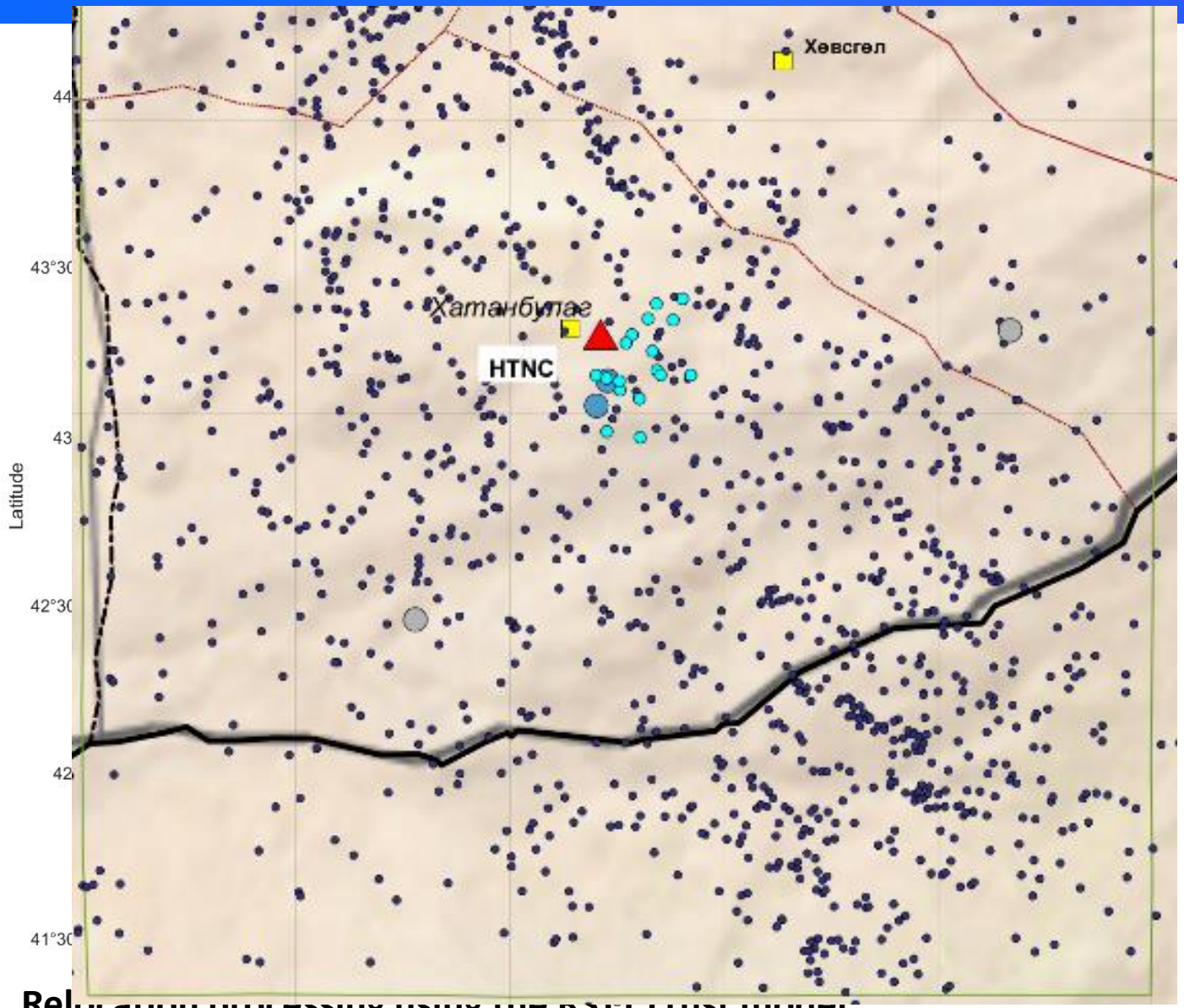

Relocation processing using the K3PT crust model

iLoc relocation

Depth distribution of iLoc relocation

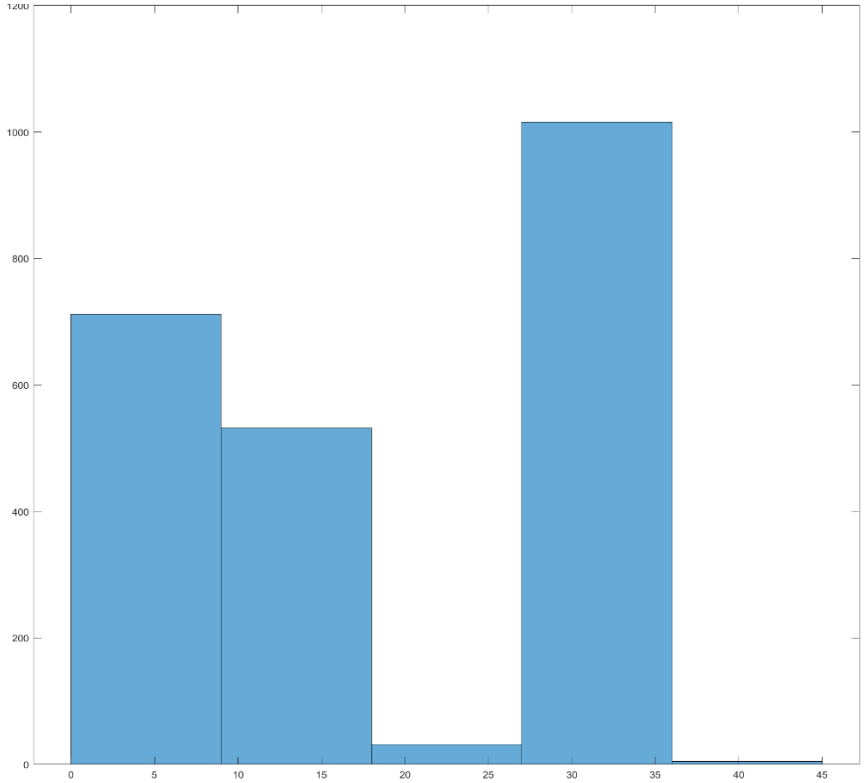

Shifted Distance of iLoc relocation

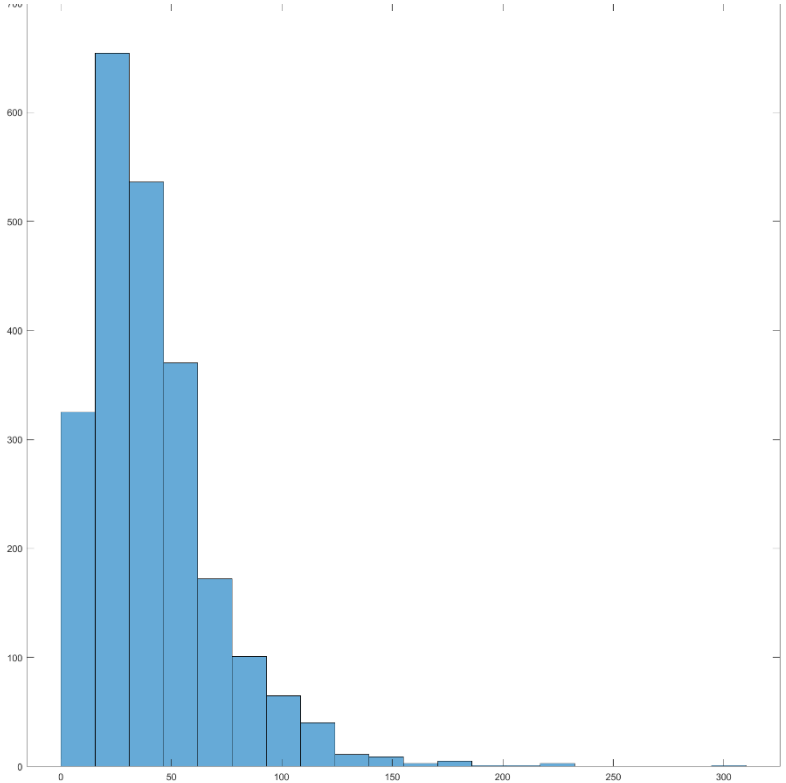

Figure: This histogram illustrates the depth distribution of earthquakes relocated using iLoc from 2015 to 2025. The events are primarily concentrated at shallow (0–10 km) and deeper levels (30–35 km), indicating a bimodal depth pattern. A notable reduction in activity around 20 km depth suggests lower seismicity in the mid-crust.

Institute of Astronomy and Geophysics

Focal mechanism of mainshock earthquake ML4.4

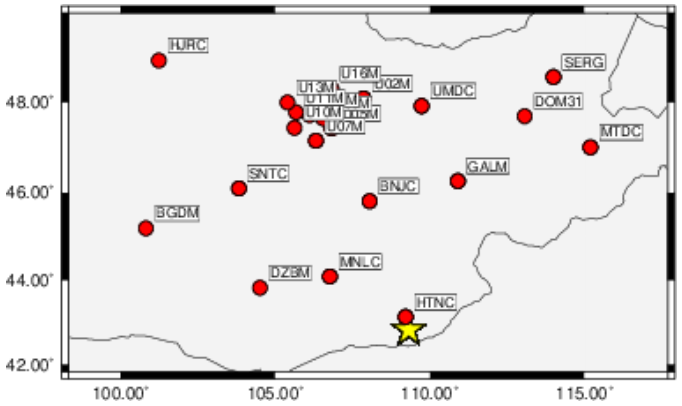

ID event	Strike	Dip	Rake	Mw	Depth
1303182	350	90	-160	4.4	12

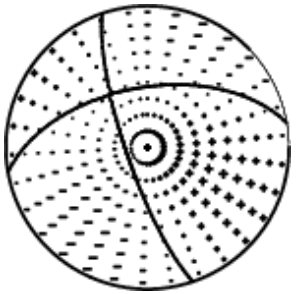

Figure. Beach ball diagram showing the focal mechanism of the earthquake. The solution was obtained using moment tensor inversion (Robert B. Herrmann, 2015).

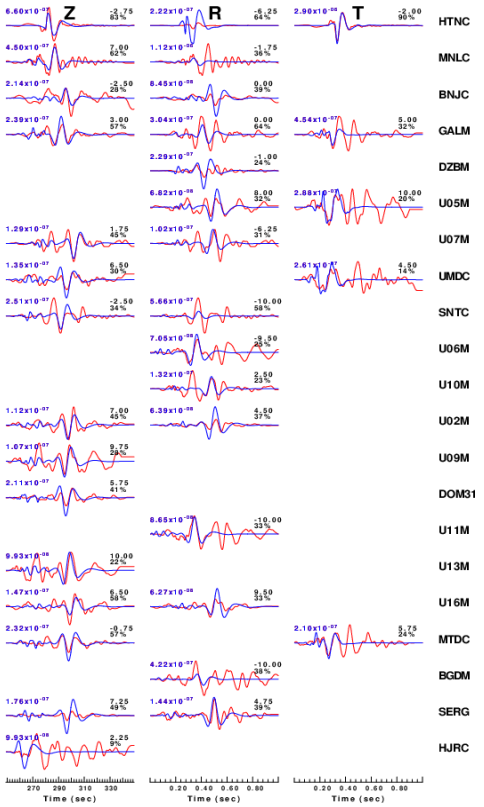

Figure. Waveform comparison at additional seismic stations for Z- and R-components (red: observed, blue: predicted).

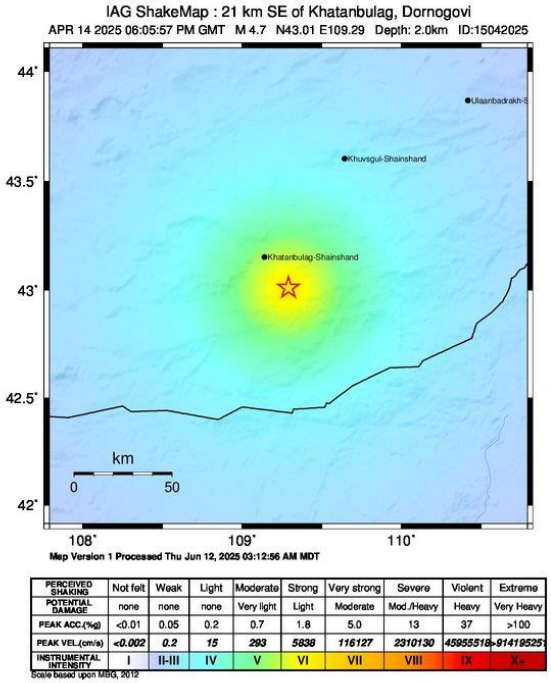

Figure. The ShakeMap application and analysis by D. Khongor. (USGS)

Institute of Astronomy and Geophysics

Focal mechanism large aftershock ML 4.2

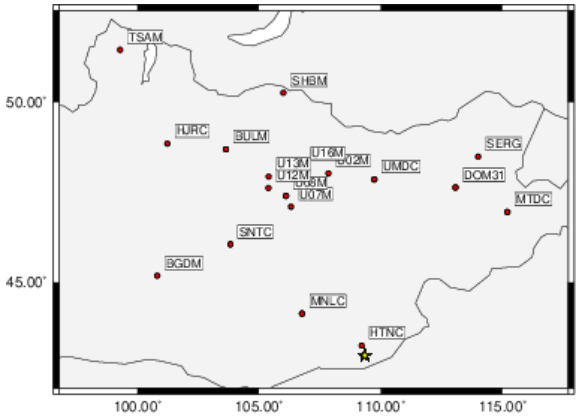

ID event	Strike	Dip	Rake	Mw	Depth
1592815	24	76	-164	4.4	15

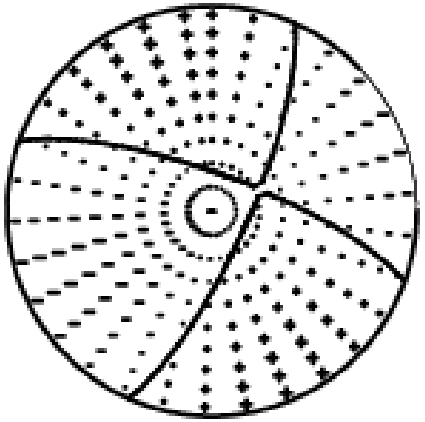

Figure. Beach ball diagram showing the focal mechanism of the earthquake. The solution was obtained using moment tensor inversion (Robert B. Herrmann, 2015).

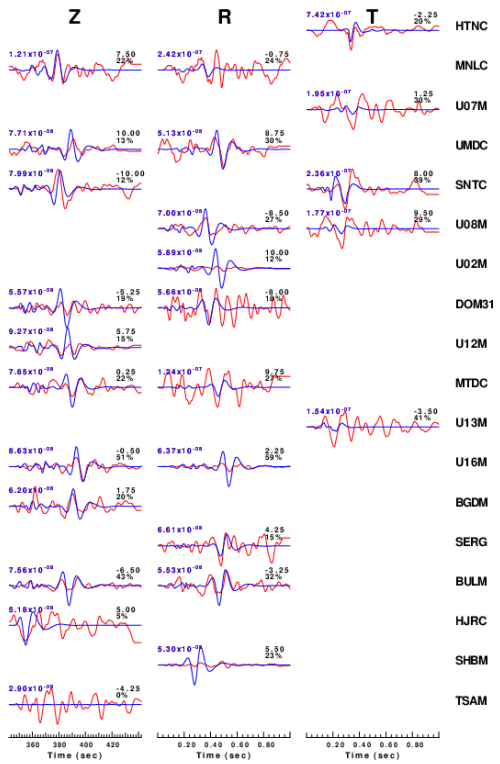

Waveform comparison at additional seismic stations for Z- and R-components (red: observed, blue: predicted).

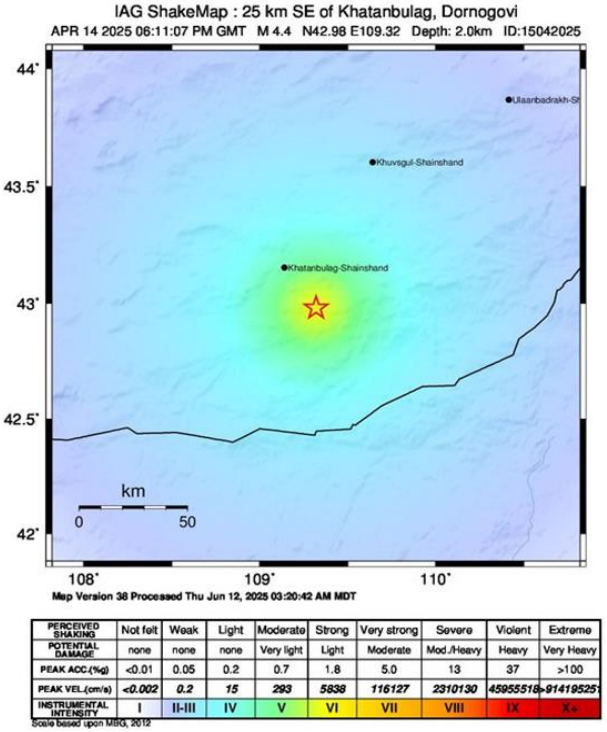

Figure. The ShakeMap application and analysis by D. Khongor. (USGS)

Institute of Astronomy and Geophysics

Focal mechanism of Large aftershock ML 3.8

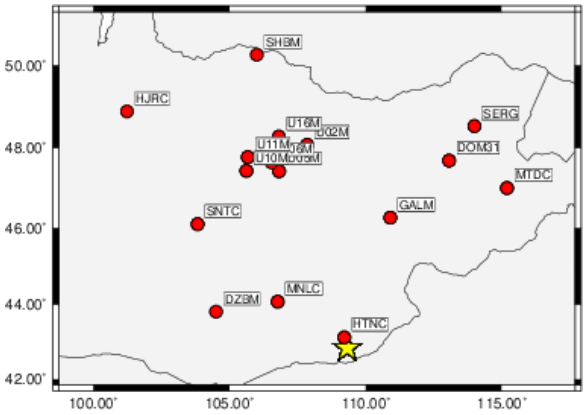

ID event	Strike	Dip	Rake	Mw	Depth
1592817	161	78	144	3.8	20

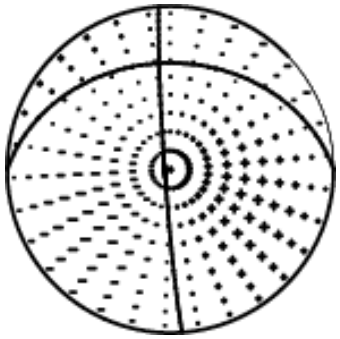

Beach ball diagram showing the focal mechanism of the earthquake. The solution was obtained using moment tensor inversion (Robert B. Herrmann, 2015).

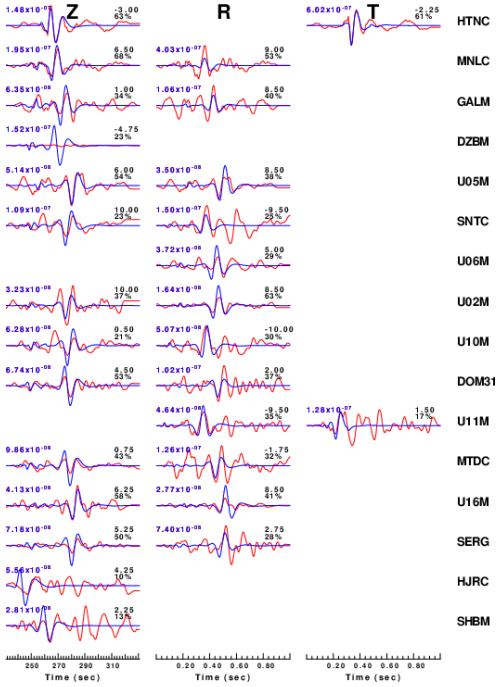

Figure. Waveform comparison at additional seismic stations for Z- and R-components (red: observed, blue: predicted).

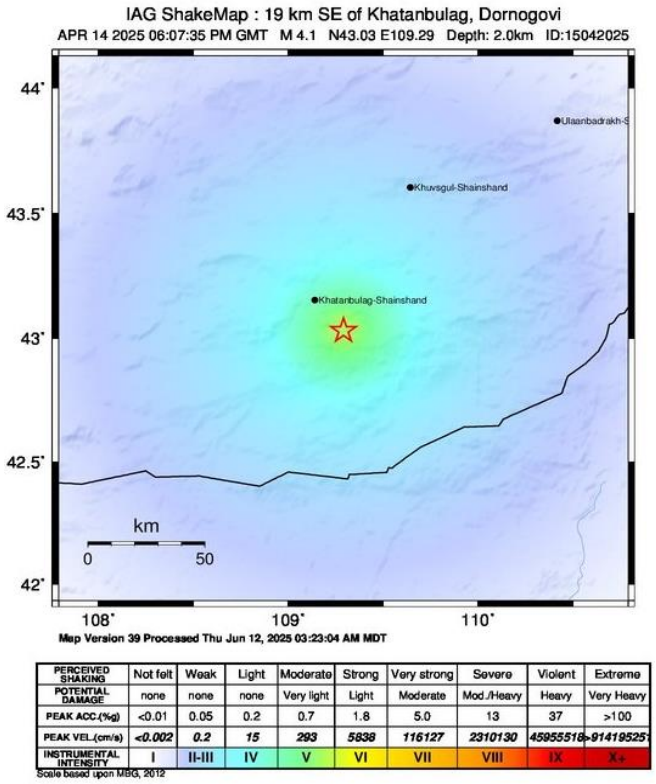

Figure. The ShakeMap application and analysis by D. Khongor. (USGS)

Institute of Astronomy and Geophysics

Conclusion

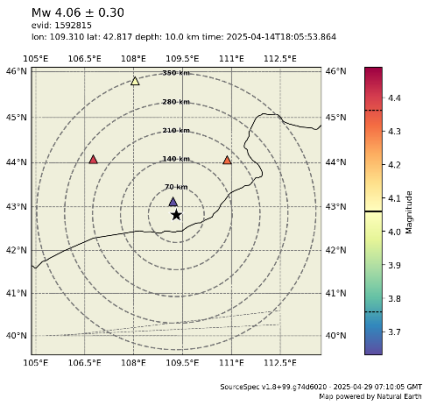

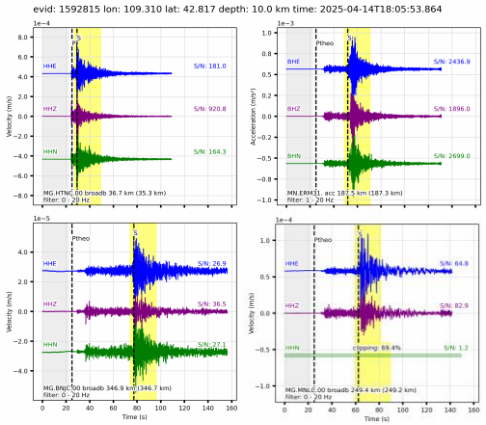

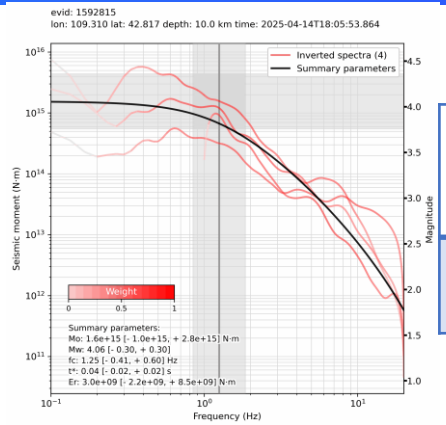

Origin time YYYY/MM/DD HH:MM:SS	ML_onyx	Mw_Ss
2025/04/14 18:05:53	4.4	4.06

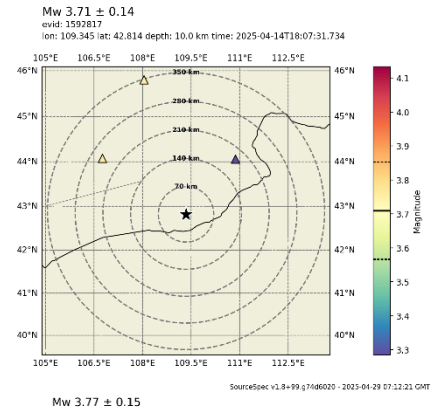

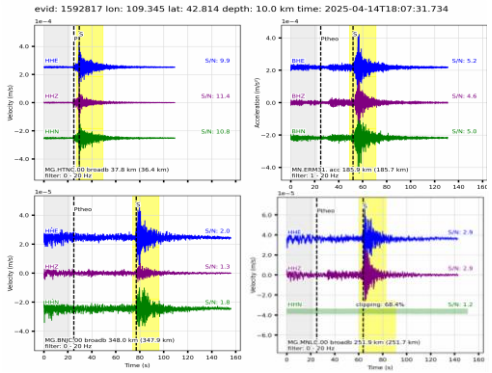

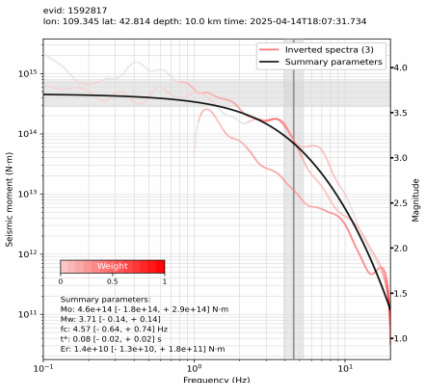

Origin time YYYY/MM/DD HH:MM:SS	ML_onyx	Mw_Ss
2025/04/14 18:07:31	4.0	3.71

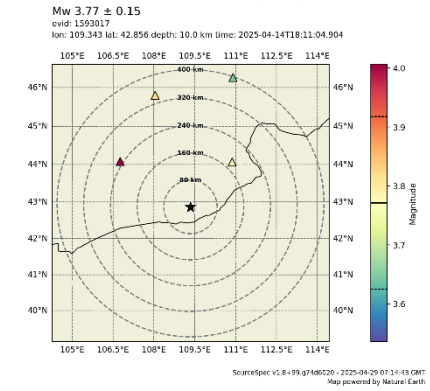

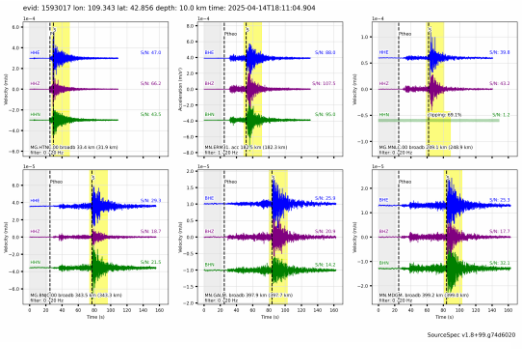

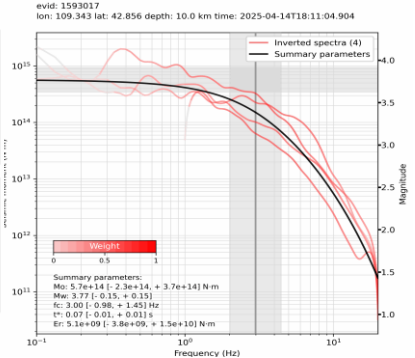

Origin time YYYY/MM/DD HH:MM:SS	ML_onyx	Mw_Ss
2025/04/14 18:11:04	4.1	3.77

Moment magnitude

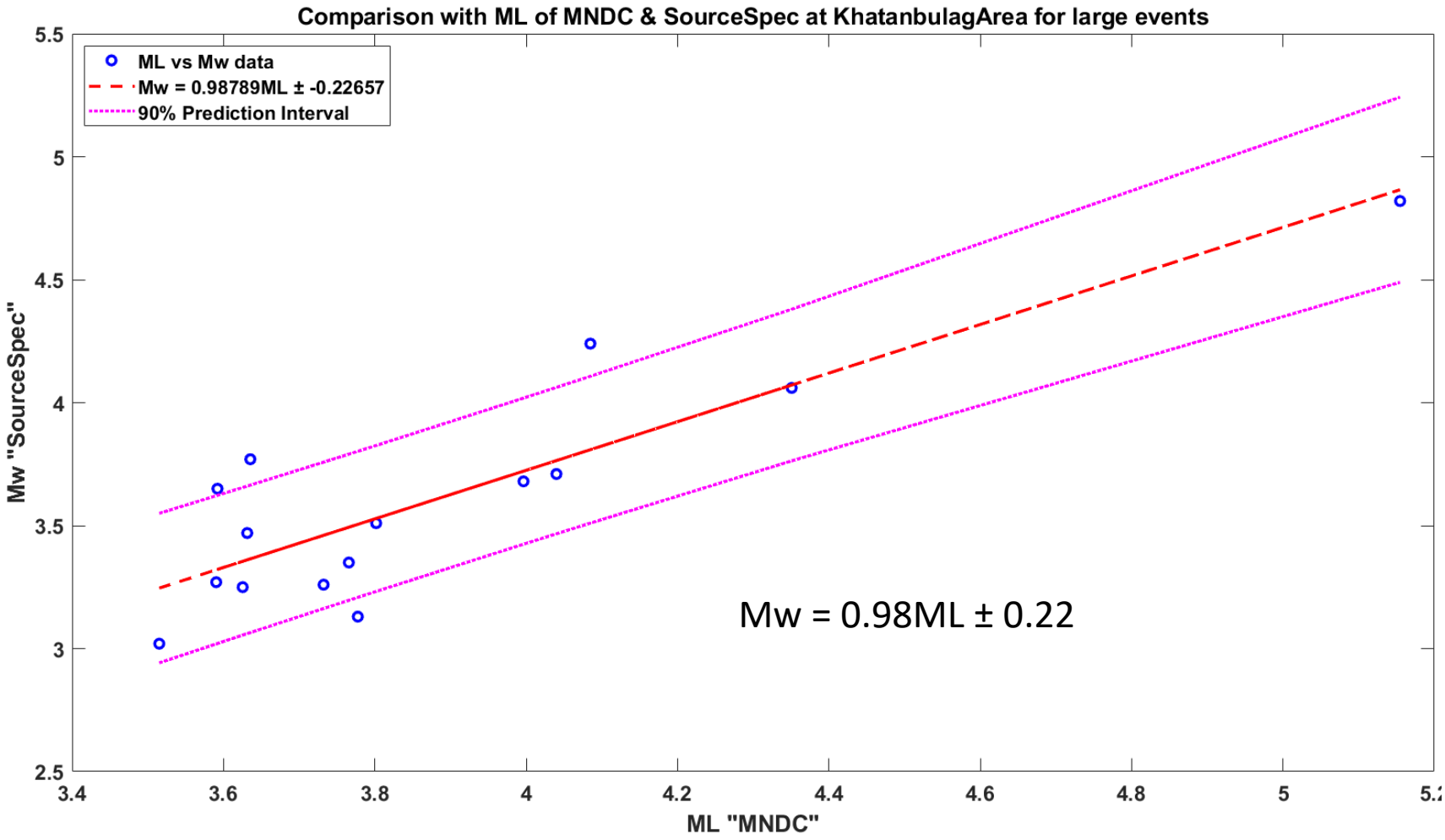

Conclusion

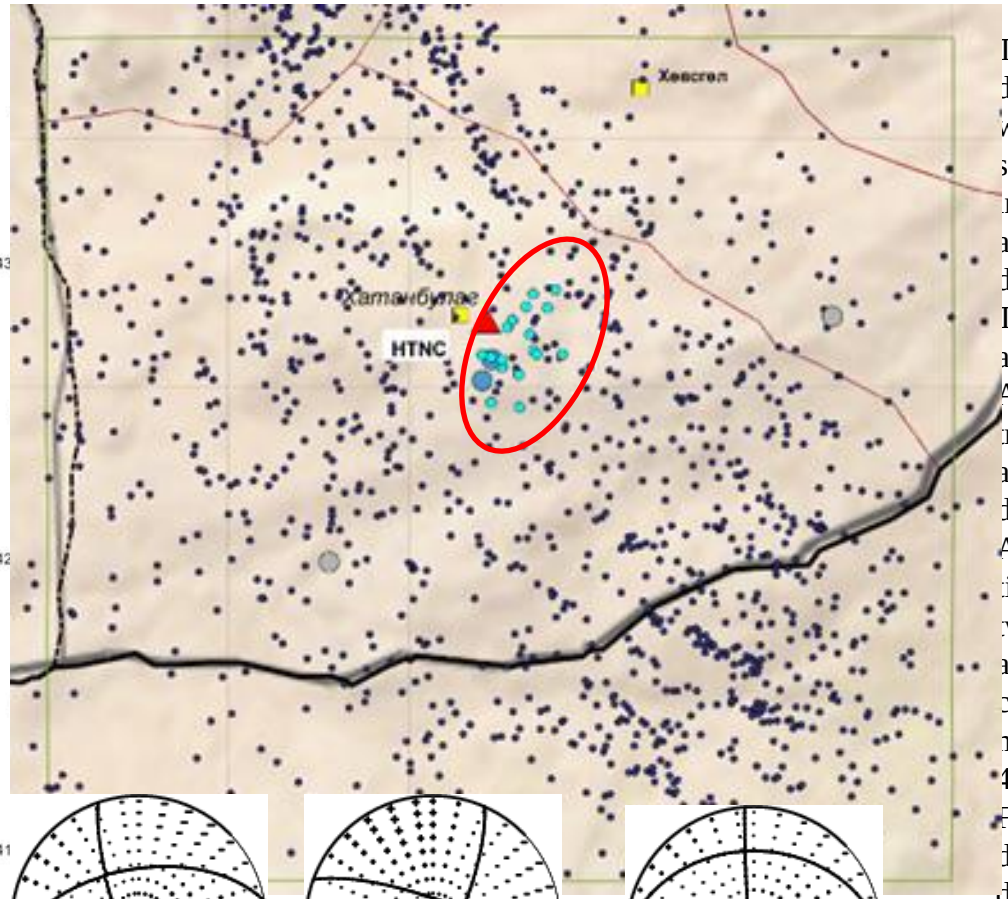

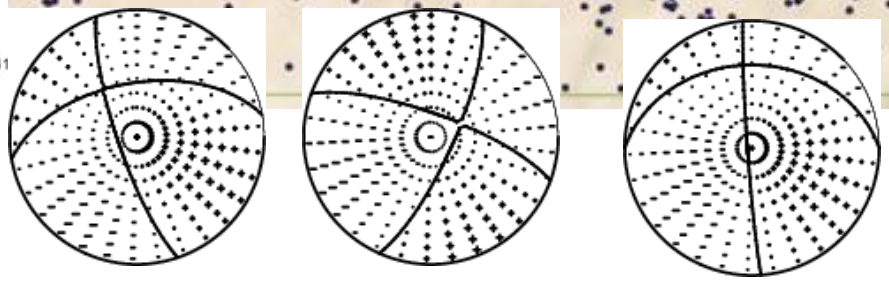

Mainshock

Two aftershock

Second aftershock

The results of the study indicate that the earthquake distribution shows an east-southeast to west-northwest trend, which in some cases corresponds to the focal mechanism solutions. In this region, the post-seismic activity was investigated using the iLoc algorithm, focal mechanism analysis, ShakeMap processing, and moment magnitude determination.

The re-location results reveal that the distribution of aftershocks and the Focal Mechanism and Second Large Aftershock exhibit a similar east-southeast to west-northwest trend. Moreover, the focal mechanism of the second large aftershock shows a comparable pattern to the overall distribution.

A magnitude 4.0 large aftershock was recorded for the first time in this area, which is notable, and it is included among two events out of the 20 aftershocks analyzed. For the study area, a lower magnitude threshold of 1.8 was selected for calculating a-value and b-value, resulting in a completeness magnitude of 1.8, with a b-value of 1.16 and an a-value of 4.87.

Figure 17 presents the aftershock distribution map, directional plot, and the focal mechanism Beach Ball diagram

Institute of Astronomy and Geophysics

a and b-value

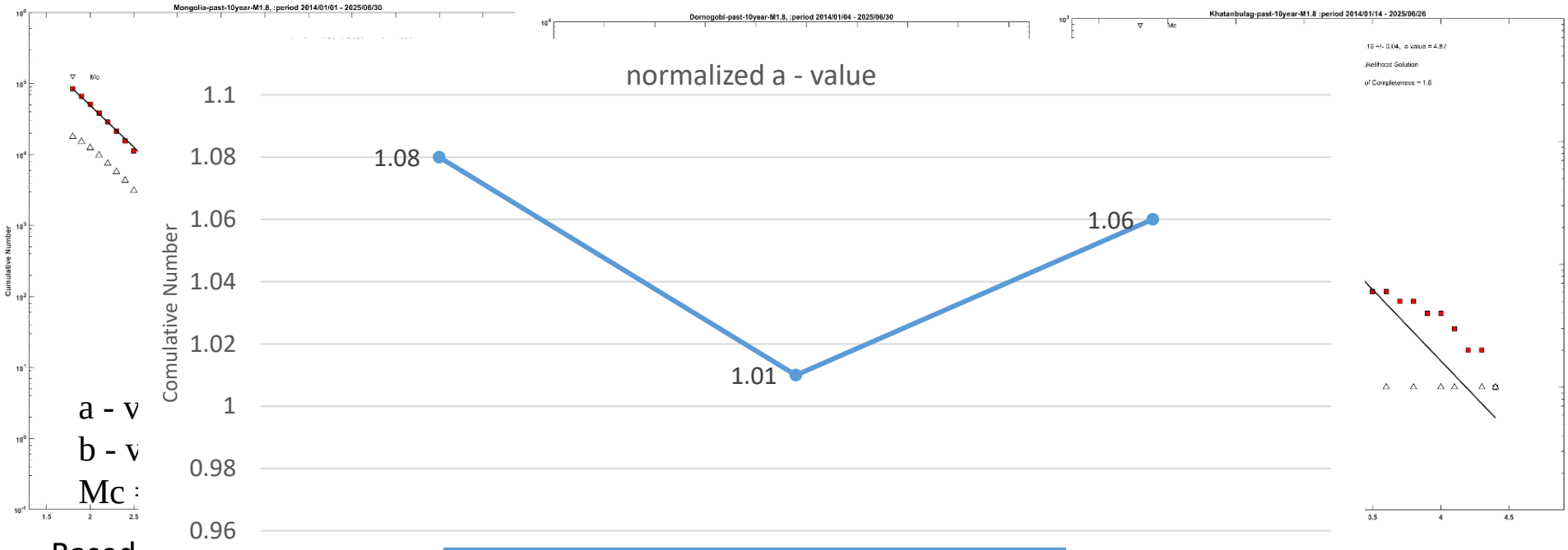

MGL Dornogobi Khatanbulag

a - v

b - v

Mc :

Based

Law (G

log N = a – b M

Where:

- N – number of earthquakes
- M - magnitude
- a = value
- b = value

We calculate a normalized ***a***-value for

$$anorm = \frac{a}{\log_{10}(Area)}$$

Area_MGL_seismic buffer_area = 2964316 km2

Area_Dornogobi_selected_area = 219198 km2

Area_Khatanbulag_targed_area = 37060 km2

THE STRONG EARTHQUAKES IN KHATANBULAG, DORNOGOBI PROVINCE

G.Bolormaa, D.Ganzorig, M. Oyun-Erdene, D. Khongor

Bolormaa.g@iag.ac.mn

Institute of Astronomy and Geophysics, MAS

ULAANBAATAR
2025.08.11